HHS Public Access

Author manuscript

Sci Transl Med. Author manuscript; available in PMC 2019 April 25.

Published in final edited form as:

Sci Transl Med. 2018 April 25; 10(438): . doi:10.1126/scitranslmed.aal1803.

Targeting protein biotinylation enhances tuberculosis chemotherapy

Divya Tiwari[1], **Sae Woong Park**[1], **Maram M. Essawy**[2], **Surendra Dawadi**[2], **Alan Mason**[4], **Madhumitha Nandakumar**[3], **Matthew Zimmerman**[4], **Marizel Mina**[4], **Hsin Pin Ho**[4], **Curtis Engelhart**[1], **Thomas Ioerger**[6], **James Sacchettini**[7], **Kyu Rhee**[3], **Sabine Ehrt**[1], **Courtney C. Aldrich**[2], **Véronique Dartois**[4,5], and **Dirk Schnappinger**[1,*]

[1]Department of Microbiology and Immunology, Weill Cornell Medical College, New York, NY, USA.

[2]Department of Medicinal Chemistry, University of Minnesota, 308 Harvard Street SE, 8-174 WDH, Minneapolis, Minnesota 55455, USA

[3]Department of Medicine, Weill Cornell Medical College, New York, NY, USA.

[4]Public Health Research Institute, New Jersey Medical School, Rutgers, The State University of New Jersey, Newark, New Jersey, USA

[5]Department of Medicine, New Jersey Medical School, Rutgers, The State University of New Jersey, Newark, New Jersey, USA

[6]Department of Computer Science and Engineering, Texas A&M University, College Station, Texas, USA

[7]Department of Biochemistry & Biophysics, Texas A&M University, College Station, Texas, USA

Abstract

Successful tuberculosis (TB) chemotherapy depends upon the unique contributions of its component drugs. Drug resistance poses a threat to the efficacy of individual agents and the regimens to which they contribute. Biologically and chemically validated targets capable of replacing individual components of current TB chemotherapy thus represent a major unmet need in TB drug development. We demonstrate that chemical inhibition of biotin protein ligase (BPL) can kill *Mycobacterium tuberculosis* (*Mtb*) and genetic silencing eliminates the pathogen efficiently from mice during acute and chronic infection. Partial chemical inactivation of BPL increases potency of two first-line drugs, rifampicin (RIF) and ethambutol (EMB), and genetic interference with protein biotinylation accelerates clearance of *Mtb* from lungs and spleens by RIF. These studies validate BPL as a vulnerable target that can serve as an alternate frontline target against *Mtb*.

Summary

*Correspondence should be addressed to dartoiva@njms.rutgers.edu or dis2003@med.cornell.edu.

Author contributions

DT, SWP, ME, SD, AM, MN, MZ, MM, HPH, and CE performed experiments. All authors contributed to experimental design and data analysis. DT, CCA, AM, VD and DS wrote the manuscript, which was edited by all authors.

Competing interests

The authors declare no competing financial interest.

One Sentence Summary

Biotin protein ligase (BPL) and protein biotinylation (PB) are druggable targets whose inhibition synergizes with rifampicin and has the potential to shorten tuberculosis chemotherapy.

Introduction

Tuberculosis (TB) is reemerging as an incurable infection due to drug-resistance. In 2013, approximately 480,000 people developed multidrug resistant tuberculosis (MDR-TB) (1). The discovery of an effective vaccine that prevents TB in adults remains an important goal but has been elusive (2). Consequently, our ability to control TB depends primarily on the development of more efficient chemotherapies for drug sensitive (DS) and drug resistant (DR) TB.

The cell envelope of mycobacteria is a selective permeability barrier containing several unique lipids which cause drug resistance and protect *Mtb* from the host immune system (*3–7*). The importance of mycobacterial lipid metabolism is underscored by the finding that over 250 genes are involved in lipid metabolism in *Mtb* as opposed to only 50 in *Escherichia coli*. The structurally diverse mycobacterial lipids are all derived from simple malonyl coenzyme A (CoA) building blocks, which are in turn prepared by acyl-CoA carboxylases (ACCs). *Mtb* encodes for three multimeric ACCs assembled from at least 10 different subunits (AccA1–3, AccD1–6, and AccE5), which together provide the malonyl-CoA, (methyl)malonyl CoA, and (long-chained alkyl)malonyl CoA building blocks required for synthesis of linear fatty acids, methyl-branched lipids, and mycolates, respectively (*8–11*). Each ACC must be post-translationally modified with the cofactor biotin (vitamin H) to become active. Blocking *de novo* biotin biosynthesis or biotin-ACC ligation, thus, has the potential to inhibit all lipid biosynthesis.

We previously reported the design and characterization of potent inhibitors of biotin protein ligase (BPL), the enzyme responsible for covalently ligating biotin onto the ACCs (*12–19*). This led to 5′-[*N*-(D-biotinoyl)sulfamoyl]amino-5′-deoxyadenosine (Bio-AMS), a BPL inhibitor with potent on-target whole-cell activity against drug-sensitive (DS) and drug-resistant (DR) *Mtb*. Nevertheless, several important questions remained concerning its mechanism of action, resistance, pharmacokinetic properties, synergy with other antitubercular drugs, and, importantly, consequences of BPL inhibition *in vivo*.

In this study, we first characterized the consequences of chemically inactivating BPL for viability of *Mtb* under different physiological conditions. Next, we determined the frequency and mechanism of resistance to BPL inactivation by Bio-AMS and used pharmacokinetic studies to characterize Bio-AMS metabolism in the host. Incomplete inhibition of BPL by fluctuating concentrations of Bio-AMS prevented growth of *Mtb* in a hollow fiber system. Furthermore, near-complete genetic inactivation of BPL killed *Mtb* during acute as well as chronic mouse infections. Finally, we established that partial genetic interference with protein biotinylation is sufficient to increase sensitivity of *Mtb* to killing by RIF during infection.

Results

Impact of chemical BPL inactivation on viability of *Mtb in vitro* and during macrophage infections

We first determined whether inhibition of BPL is sufficient to kill *Mtb*. INH, a first-line drug that inhibits the synthesis of mycolic acids (20), was used as a control. In biotin-free media, the BPL-inhibitor Bio-AMS was bactericidal at a concentration of approximately 5-fold the minimal inhibitory concentration (MIC) and killed *Mtb* with kinetics similar to that of INH (Fig. 1A). After 10 days of drug exposure, INH resistant mutants appeared whereas Bio-AMS continued to reduce colony-forming units (CFU) until viability of the culture was below the limit of detection of 25 CFU/mL.

The anti-mycobacterial activity of several small molecules depends strictly on the primary carbon source used to cultivate *Mtb* (21). However, changes in the primary carbon source had little impact on the MIC (Fig. 1B) or the minimal bactericidal concentration (MBC, Fig. S1A) of Bio-AMS. Addition of biotin to the growth medium increased the MIC only 4-fold (Fig. S1B), but when we analyzed Bio-AMS with *Mtb* that had ceased to replicate due to starvation in phosphate-buffered saline (PBS) we observed no reduction in viability (Fig. S1C). In macrophages Bio-AMS inhibited growth of *Mtb* in a concentration dependent manner (Fig. 1C) and a tetrazolium reduction assay did not detect toxicity for macrophages (Fig. S1D). Bio-AMS also showed no signs of mitochondrial toxicity (Fig. S2).

Thus, chemical inactivation of BPL kills growing *Mtb* independent of the carbon source the bacteria are consuming and prevents the growth of intracellular *Mtb*, but is inactive against PBS-starved *Mtb*.

Resistance to chemical BPL inactivation

Bio-AMS resistant *Mtb* was isolated with a frequency of ~1 in 10^7 CFU when Bio-AMS was present at a concentration of 10× the MIC (Fig. 2A). This frequency decreased to less than 1 in 10^8 at 25× the MIC and we did not isolate any resistant *Mtb* from 10^8 CFU at 50× the MIC of Bio-AMS. For INH we observed a resistance frequency of approximately 1 in 2.5×10^6 CFU, which did not vary much with drug concentration. The Bio-AMS resistant clones expressed wild type amounts of BPL (Fig. S3A) and were free of mutations in *birA*, the gene encoding BPL. Whole-genome sequencing revealed all resistant isolates to contain mutations in *rv3405c*, most of which were predicted to inactivate *rv3405c*, and three strains harbored mutations only in *rv3405c* (Table S1). Rv3405c is a transcriptional repressor that controls *rv3406* in *M. bovis* BCG (22). When we compared mRNAs from Bio-AMS resistant isolates with mRNA from WT, we detected a drastic change in *rv3406* (Table S2), which resulted in overexpression of Rv3406 (Fig. S3B). *Mtb* carrying an Rv3406 overexpression plasmid (pGMEH-Ptb38-rv3406) was 64-fold more resistant to Bio-AMS than WT (Fig. 2B). We concluded that overexpression of Rv3406 is sufficient to cause Bio-AMS resistance.

Rv3406 is a dioxygenase that oxidizes 2-ethylhexyl sulfate (2-EHS, Fig. S3C) and its activity requires non-heme iron (II) and alpha-ketoglutarate (α-KG) (23). To test if Rv3406 could also oxidize Bio-AMS, we incubated Bio-AMS with recombinant Rv3406 and α-KG.

This resulted in the time dependent formation of an UV-active product (Fig. 2C) with a λ_{max} of 254 nm and a molecular weight of 265, which are both consistent with the adenosine 5′-aldehyde **3** (Fig. S3D). This compound likely arises through oxidation of Bio-AMS at C-5′ of the nucleoside and spontaneous disproportionation of the resultant intermediate hemiaminal **2** into aldehyde **3** and *N*-(biotinoyl)sulfamide **4** (Fig. S3D). Rv3406 thus oxidizes Bio-AMS in the same manner it oxidizes an alkyl sulfate. This mechanism for enzymatic reactions of alkyl sulfates catalyzed by α-KG dependent dioxygenases is well established (23) and the identity of metabolite **4** was confirmed with an authentic standard (Fig. S3E). Steady-state kinetic analysis revealed that Bio-AMS is a poor substrate of Rv3406 and has a 48-fold higher K_M value and nearly 1,300-fold lower k_{cat} value than 2-EHS (Table S3). Nevertheless, degradation of Bio-AMS was dependent on the enzymatic activity of Rv3406 as degradation only occurred in the presence of α-KG (Fig. 2C). Furthermore, we found that the amount of Bio-AMS in *Mtb* was inversely correlated with expression of Rv3406 (Fig. S4A). Consistent with the *in vitro* data, we also measured higher amounts of *N*-(biotinoyl)sulfamide **4** when Rv3406 expression was increased (Fig. S4B). Collectively, these results demonstrated that the most frequent mechanism of spontaneous resistance to chemical inactivation of BPL is enzymatic cleavage of Bio-AMS.

BPL as a target to control *Mtb* infections

In mice, Bio-AMS was rapidly eliminated, in part due to hydrolysis at the acyl-sulfamide linkage, (Fig. S5, S6 and Table S4). In addition, the dose of Bio-AMS required to achieve concentrations above the MIC for a substantial fraction of the dosing interval was not tolerated by mice (Table S5). We therefore employed (i) a hollow fiber bioreactor system (HFS) to evaluate the impact of fluctuating Bio-AMS concentrations on growth of *Mtb* and (ii) a genetic approach to determine the consequences of inactivating *Mtb*'s BPL during infections.

In the HFS, medium is pumped from a central reservoir (CR) through a cylindrical bioreactor filled with tubular, semi-permeable membrane fibers. By manipulating the flow rate through the system, one can increase or decrease the drug concentrations to which the bacteria are exposed, creating defined, dynamic pharmacokinetic (PK) drug profiles (24). The fiber pore size (0.4 μM) ensures that the bacteria introduced into the bioreactor cartridge are retained in the extracapillary space (ECS). A log phase culture of *Mtb* H37Ra was introduced into an HF cartridge, allowed to grow in 7H9 for two days and then challenged with Bio-AMS. The Cmax was chosen to maintain concentrations above MIC90 for most of the dosing interval. The clearance flow rate was set to achieve a half-life for Bio-AMS of between 9 and 10 hours, which is a typical half-life of several antibiotics in clinical use (*25, 26*). The PK profiles of Bio-AMS were measured in both the CR and the ECS. Profiles taken on days 0 and 14 showed Cmax values of ~32 μM in the CR and ~17 μM in the ECS (Fig. 3A). Viability of *Mtb* H37Ra was monitored by CFU enumeration, which showed that Bio-AMS prevented growth in the HFS (Fig. 3B). The culture remained free of *Mtb* H37Ra resistant to Bio-AMS for 15 days, but resistant mutants emerged at around day 18. The appearance of Bio-AMS resistant *Mtb* H37Ra suggests that the PK profile analyzed here may lead to a higher frequency of resistance than observed in selections on agar plates. In the future, it will thus be important to define how PK parameters influence the frequency

and type of mutations leading to resistance. Nevertheless, using Bio-AMS at a peak concentration and half-life similar to those of other clinically used cell wall-targeting antibiotics, the HFS simulations revealed that incomplete chemical inhibition of BPL achieves static growth inhibition across the dosing interval.

Next, we used a previously described dual-control switch (*27, 28*) to construct an *Mtb* mutant, BPL-DUC, in which anhydrotetracycline (atc) induces both transcriptional silencing of *birA* and proteolytic inactivation of BPL (Fig. S7). Exposure of BPL-DUC to atc (i) depleted BPL below the limit of detection of immunoblots within 24 h (Fig. S8A), (ii) caused a decrease in biotinylated proteins (Fig. S8B), (iii) prevented growth (Fig. 4A), and (iv) decreased viability of *Mtb* (Fig. 4B). C57BL/6 mice were infected with BPL-DUC and fed the mice doxycycline (doxy) containing food either from the beginning of the infection, after 14 days, after 35 days or not at all (Fig. 4C, d). Mice that were infected with H37Rv and received doxy-supplemented food served as a control. As early as 14 days post infection, we failed to recover CFU for BPL-DUC from the lungs of mice that received doxy throughout the infection (Fig. 4C). Similarly, when doxy food was given during the acute infection (i.e. on day 14), we also did not recover any CFU two weeks later. When BPL was inactivated during the chronic phase by switching to doxy food on day 35 we observed a decrease in CFU of more than 2 $\log_{10}$ by day 56 and lungs were free of CFU by the next time point (day 112). On day 169 post-infection, we did not recover CFU from any of the groups that received doxy-supplemented food (Fig. 4C). Decreases in CFU that occurred after doxy treatment were accompanied by reduced lung tissue pathology (Fig. S9). Depleting BPL had a similar impact on CFU in spleens as it had in lungs (Fig. 4D). We conclude that depletion of BPL kills replicating *Mtb in vitro* and efficiently eliminates viable *Mtb* from mice during acute and chronic infections.

Importance of *Mtb* protein biotinylation for the activity of rifampicin, isoniazid and ethambutol

The cell envelope of mycobacteria is a highly selective barrier that contributes greatly to the intrinsic drug resistance of *Mtb* (*3, 4*). The integrity of this envelope requires fatty acids and lipids, which depend on biotinylated ACC enzymes for synthesis. We therefore analyzed how inhibition of protein biotinylation affects *Mtb*'s acid fastness and susceptibility to RIF, INH and ethambutol (EMB). First, we treated *Mtb* with a lethal dose of Bio-AMS and analyzed the cell envelope using acid-fast staining before and after the amounts of biotinylated proteins were reduced (Fig. S10). This detected an increase in acid-fast negative bacteria on day 5 post exposure (when biotinylated proteins just began to decrease) and after 10 days of exposure to Bio-AMS most bacteria stained as acid-fast negative. Next, we measured if a sublethal dose of Bio-AMS changes susceptibility of *Mtb* to RIF, INH, and EMB. As it takes several days before exposure to Bio-AMS affects *Mtb*'s protein biotinylation pattern, we first grew *Mtb* with and without Bio-AMS for three days and then exposed these cultures to RIF, INH, or EMB – in each case, with or without Bio-AMS. Sublethal doses of Bio-AMS reduced the MIC of RIF and EMB but left the MIC of INH unchanged (Fig. 5ABC). We then determined if Bio-AMS could also enhance the cidal activity of RIF and EMB. For these experiments, we used Bio-AMS at 1 μM, RIF at 6.5 nM, and EMB at 12.5 μM. As expected, none of the compounds were cidal at these

concentrations when used individually (Fig. 5DE). However, the combined use of either rifampicin or ethambutol with Bio-AMS killed more than 99.7 and 99.9% of the inoculum after 20 days of treatment.

We next asked if the increased potency of RIF and EMB caused by Bio-AMS could be replicated by limiting access to biotin. We grew the biotin auxotroph *Mtb* Δ*bioA* in media with defined biotin concentrations and measured the MIC of EMB and RIF. This showed that decreasing concentrations of biotin decreased the MIC of RIF but left the MIC of EMB unchanged (Fig. S11AB). When we compared the amount of RIF that accumulated in WT and *Mtb* Δ*bioA* we found increased amounts of RIF in *Mtb* Δ*bioA* when the mutant was grown with low amounts of biotin (Fig. S11C). Thus, Bio-AMS improves the potency of RIF by interfering with synthesis of a normal cell envelope, as indicated by the reduction in acid fastness, which in turn facilitates RIF uptake. In addition, Bio-AMS decreases the MIC of EMB by a yet to be determined mechanism.

Interfering with protein biotinylation enhances the activity of RIF during *Mtb* infection

Together with INH, RIF forms one of the cornerstones for treatment of drug-sensitive TB. We therefore sought to determine if sublethal interference with *Mtb* protein biotinylation could also improve the potency of RIF during infections. It would have been practically impossible to answer this question using BPL-DUC because this mutant is cleared rapidly from mice at the standard dose of doxy and the dose-response curve of the DUC switch is so steep (28) that it is infeasible to identify a dose of doxy that leads to intermediate silencing in animals. In previous work, however, we had constructed a panel of *bioA*-TetON mutants, in which transfer from media containing atc or doxy to atc/doxy-free media silences expression of BioA to different degrees (29). One of these mutants, *bioA* TetON-1, expresses ~1,000% BioA with atc and ~5% BioA without atc compared to WT, but grows almost like WT without supplemental biotin (29). We therefore measured RIF sensitivity of *bioA* TetON-1 and found the mutant to be more sensitive than WT to RIF without atc and more resistant than WT with atc (Fig. 6A).

Next, we infected C57BL/6 mice with *bioA* TetON-1 by aerosol and divided the mice into two groups, one of which received doxy-supplemented food while the other was fed doxy-free food. Twenty-one days post infection, RIF was administered by oral gavage 5 days a week at a dose of 10 mg/kg for either 4 weeks or 8 weeks. At the end of RIF treatment, the mice were kept without RIF for 3 days and then CFU were determined in lungs and spleens. In agreement with our previous experiments, there was no difference in bacterial titer obtained from groups on doxy or regular chow diet in the absence of RIF, which demonstrates that the strain can sustain infection in mice even after expression of BioA is reduced (Fig. 6BC). Both treatment groups showed progressive reduction of CFU after rifampicin treatment as compared to the controls at 4 weeks and 8 weeks. However, significantly fewer CFU ($p < 0.05$) were obtained from the lungs of mice when BioA expression was reduced due to the lack of doxy than when BioA was expressed constitutively (Fig. 6B). Similar results were obtained for the spleens of these mice (Fig. 6C). Importantly, without doxy, treatment with RIF alone was sufficient to kill *Mtb bioA*

TetON-1 in lungs by more than 200-fold within 4 weeks. This efficacy is similar to that achieved by combining RIF with INH (*30, 31*).

To test if doxy could have indirectly changed exposure of RIF, we performed a drug-drug interaction study in which RIF was administered with and without doxy to uninfected mice, and measured both doxy and RIF plasma concentrations following a single RIF dose and at steady state. Seven daily doses of RIF caused a small but statistically significant decrease (~30%, $p<0.05$) of doxy exposure over the 8 h period during which plasma concentrations were measured. However, RIF exposure was not affected by co-administration of doxy (Table S6). In addition, drug distribution studies with doxy administered in the diet to *Mtb*-infected rabbits showed that doxy accumulates in lung lesions relative to plasma, with lesion/plasma ratios ranging from approximately 4 to 6 (Table S7). Accumulation into tissue was independent of the doxy concentration in the diet (200 or 400 ppm). Thus doxy concentrations in lung lesions are at least as high as those measured in plasma.

Taken together, these experiments demonstrate that interfering with *Mtb*'s ability to biotinylate proteins increases sensitivity to RIF and strongly suggest that Bio-AMS or other inhibitors targeting biotin metabolism will be excellent drug candidates that can be expected to synergize with RIF in vivo.

Discussion

Tuberculosis remains a major killer in the developing world. The stop TB partnership envisions a TB free world by 2050 (1). Continued improvement of TB chemotherapy including the development of new drugs will be required to achieve this goal. New TB drugs should ideally be active against DS and DR *Mtb* and shorten the treatment of DR and DS TB. *Mtb* BPL was shown to be susceptible to chemical inhibition by Bio-AMS, which can prevent growth of DS and DR *Mtb* (17). This suggested *Mtb* BPL as a potentially attractive target for TB drug development, but its importance for bacterial viability under different physiological conditions and during infections remained to be determined. It also remained unclear how inhibition of BPL impacts the potency of current first line drugs and how it might affect the length of treatment. By answering these questions, we sought to further evaluate the potential of Bio-AMS as a lead and BPL as a target for TB drug development.

We found chemical inhibition of BPL to (i) be cidal for *Mtb* during growth with different carbon sources (Fig. 1AB, Fig. S1A), (ii) prevent growth in macrophages (Fig. 1C, Fig. S1C), (iii) have a low frequency of low-magnitude resistance and an undetectable frequency of high-magnitude resistance (Fig. 2A), (iv) prevent growth of *Mtb* in HFS simulating fluctuating Bio-AMS concentrations typically observed in *in vivo* systems (Fig. 3), and (v) synergize with other TB drugs (Fig. 5AB). To determine the consequences of BPL inhibition during infections we constructed *Mtb* BPL-DUC (Fig. S7), which enabled rapid depletion of BPL by means of a genetic approach (Fig. S8A). Characterization of this mutant confirmed our conclusions from chemical BPL inactivation experiments and revealed that depletion of BPL is sufficient to rapidly kill *Mtb* during acute and chronic infection in mice (Fig. 4CD, Fig. S9). Interestingly, depletion of BPL eradicated *Mtb* not only during acute infections but also if it was initiated on day 35 after the bacteria had already established a chronic

infection. This is in contrast to both the lack of Bio-AMS activity against nonreplicating *Mtb in vitro* and the potency of INH, which is higher if administered during the acute phase (e.g. beginning on day 3 post infection) rather than during the chronic phase (e.g. beginning on day 28 post infection) (32). That BPL inactivation efficiently kills *Mtb* during the chronic phase of mouse infection is consistent with data demonstrating that *Mtb* is still replicating during this stage of the infection even though the CFU count remains stable (33). Moreover, it suggests that BPL might also be required for ACCases to synthesize the building blocks for the cell wall remodeling that seems to occur during chronic infection (34).

One main limitation of the work that characterized *Mtb* BPL so far is that it did not yet lead to a drug-like inhibitor with sufficient bioavailability. It thus seems worth noting that susceptibility to cleavage at the biotin-adenosine linker both contributes to its limited bioavailability and is the primary mechanism of spontaneous resistance to Bio-AMS. Ongoing experiments that aim to improve bioavailability of Bio-AMS therefore should focus on modifications that enhance the stability of the acyl-sulfamide linker region of the molecule connecting the biotin and nucleoside moieties or analogues wherein the acyl-sulfamide is replaced with a suitable bioisostere. Using this approach, it may be possible to not only improve bioavailability, but to also further decrease the frequency of resistance by overcoming Rv3406-mediated destruction of Bio-AMS. The enzyme(s) that cleaves Bio-AMS in mice also remains unknown; however, we were able to identify the alkyl sulfatase Rv3406 as the enzyme responsible for Bio-AMS degradation in *Mtb*. Interestingly, Cole and co-workers have shown that an unrelated class of 2-carboxyquinoxalines that target DprE1 are also inactivated by Rv3406, but via an alternative mechanism whereby the compounds mimic the substrate α–KG (35). This suggests that Rv3406 enzyme may have a more general role in xenobiotic metabolism.

Successful therapy of TB depends on drug combinations and new drugs should ideally synergize with the existing frontline drugs. Partial inhibition of BPL by sublethal concentrations of Bio-AMS increased the potency of RIF and EMB, revealing a very attractive feature of BPL as a target for TB drug development (Fig. 5). Limiting *Mtb*'s access to biotin also allowed us to determine how reducing *Mtb* protein biotinylation affects the potency of RIF during infections. This showed that partial inhibition of *Mtb* protein biotinylation, which by itself did not reduce growth of *Mtb* in lungs, accelerated killing of *Mtb* by RIF in mice (Fig. 6BC). The magnitude of this effect is noteworthy. The potency we observed for treatment of an *Mtb* mutant with impaired protein biotinylation by RIF alone is similar to the potency reported for treatment of WT *Mtb* by the combination of RIF with INH (*30, 31*).

RIF and INH are two of the most important drugs for treatment of TB. INH has the most potent bactericidal activity during the early treatment and RIF is most effective in preventing relapse (*36–38*). This importance of the INH and RIF combination is evidenced by the fact that TB caused by *Mtb* that is resistant to INH and RIF is classified as multidrug-resistant (MDR), irrespective of resistance to other drugs. Inactivation of BPL resembles inhibition of InhA, the target of INH, in that both interfere with cell envelope biosynthesis and kill growing *Mtb* rapidly both *in vitro* and during infections. Potentially, drugs targeting *Mtb*

BPL might be as effective as INH for treating TB and could help to further shorten TB chemotherapy by improving the potency of RIF.

Materials and Methods

Study design:

The overall objective of this study was first to provide a more thorough evaluation of the previously described BPL inhibitor Bio-AMS and then to further validate *Mtb*'s BPL as a target for TB drug development. Bio-AMS was characterized with respect to its activity under a variety of growth conditions, primary mechanism of resistance, pharmacokinetic properties, and interaction with existing TB drugs. Genetic approaches were applied to evaluate BPL as a target for drug development by determining the consequences of depleting BPL *in vitro* and during infection. Animals were randomly allocated into groups and identifiable with respect to their treatment during the experiments. All studies were carried out in accordance with the guide for the fair and ethical use of Laboratory Animals of the National Institutes of Health, with approval from the Institutional Animal Care and Use Committee (IACUC) of the New Jersey Medical School, Rutgers University, Newark or the IACUC of Weill Cornell Medical College. Animals were maintained under pathogen-free conditions and fed water and chow *ad libitum*; all efforts were made to minimize suffering or discomfort. All experiments with *Mtb* were carried out in biosafety level 3 facility and approved by the relevant institutional biosafety committees.

Materials and Reagents:

Middlebrook's 7H9 medium, 7H10 medium and Middlebrook OADC (oleic albumin dextrose catalase) growth supplement were from Difco. Hygromycin (Thermofisher Scientific) Kanamycin (Sigma) and Zeocin (Invitrogen) were used at a concentration of 50 μg/mL, 25 μg/mL and 25 μg/mL respectively. Anti-BPL antiserum was generated using purified BPL protein by Covance and used at a dilution of 1:2,500. Anti-rv3406 antiserum was a kind gift from Dr. Leila de Mendonça Lima and used at a dilution of 1:1,000. Strains are listed in Table S8.

Antibacterial activity measurements:

MIC measurements were performed as described (18); CFUs were used as a readout to assess bactericidal activities in liquid culture and during infections of bone marrow derived macrophages. Carbon sources were used at a concentration of 0.1%. PBS starvation was used as a model for nonreplicating bacteria as described previously (28).

Bio-AMS resistance:

Approximately 10^8 bacteria were cultured on 7H10 agar plates containing drug at a concentration of 10×, 25× or 50× the MIC. Frequency of resistance was calculated as number of CFUs/10^8 bacteria plated. mRNA analyses of Bio-AMS resistant strains were performed as described in our previous work (39).

Mouse infection with *Mtb* BPL-DUC and *bioA* TetON-1:

4–6-week-old female C57BL/6 mice were infected with ~100 CFUs of BPL-DUC strain and divided into various groups. The control group was maintained on a regular diet whereas test groups received 2000 ppm doxy rodent chow (Research Diets, St. Louis, MO) when indicated. At each time point 4 mice per group were sacrificed, lung and spleen were homogenized in PBS, and dilutions were cultured on antibiotic-free agar plates. C57BL/6 mice were infected with *bioA* TetON-1 as for BPL-DUC. The control group received doxy throughout the experiment; the test group received the regular chow. RIF was administered at a dosage of 10 mg/kg by oral gavage 5 days a week. 8 mice from each group were sacrificed 4 and 8 weeks after RIF treatment and organs processed as described above.

Pharmacokinetic profiling:

Groups of 4 mice received Bio-AMS formulated in 0.9% saline according to the following dosing scheme: 5 mg/kg via the intravenous (IV) route, 25 mg/kg via the intraperitoneal (IP) route and 25 mg/kg via the oral (PO) route. Blood samples were collected in heparinized tubes, pre-dose and 5 min, 15 min, 30 min, 1 h, 1.5 h, 3 h, 5 h, and 8 h post-dose following IV and IP injections, and pre-dose, 5 min, 30 min, 1 h, 3 h, 5 h, and 8 h following oral gavage. Blood samples were centrifuged to recover plasma and quantify Bio-AMS and its major metabolites by LC/MS-MS as described in the supplementary materials.

Tolerability:

Groups of 3 mice received either 50 mg/kg, 100 mg/kg, 250 mg/kg or 500 mg/kg of Bio-AMS via intraperitoneal injection at 4 mL/kg. They were observed continuously for the first half hour post injection, then at 24 h post-injection.

Biochemical characterization of Rv3406:

His-tagged Rv3406 was overexpressed in BL21 (DE3) *E. coli*, purified as described (23). Enzymatic activities were established as described in the supplementary materials.

Intra-bacterial pharmacokinetics:

A previously described (28) experimental set up was used to study accumulation of Bio-AMS and its degradation products inside *Mtb*. Briefly, *Mtb* laden filters were grown in Middlebrook 7H10 agar plates for 5 days followed by exposure to Bio-AMS for 18 h in GAST medium containing 25 μM Bio-AMS or an equivalent amount of DMSO. After 18 h the filters were incubated on GAST medium for 24 h without any antibiotics and samples were collected and processed as described in the supplementary materials.

Activity of Bio-AMS in a hollow fiber bioreactor system (HFS):

Mtb H37Ra (ATCC 25177) was grown in Middlebrook 7H9 medium supplemented with OADC for 4 days at 37°C. High flux polysulfone HF cartridges (C2011, FiberCell Systems Inc., New Market, MD 21774) were equilibrated for 3 days with 7H9 OADC. Initial PK data was obtained for Bio-AMS diluted in 7H9 OADC and infused by syringe pump into the HFS. A clearance flow rate was used that simulated a Bio-AMS half-life of 9 to 10 hours in the ECS. To determine the susceptibility of H37Ra to Bio-AMS under defined PK

parameters, a new HF cartridge pre-equilibrated with 7H9 OADC was inoculated with 20 mL of a bacterial suspension of 10^4 to 10^6 CFU/mL. The culture was allowed to establish in the cartridge ECS (extra-capillary space) under a constant flow of 7H9 OADC (30 mL/h) for 2 days before the first Bio-AMS infusion. To achieve a Cmax of at least 9 μM in the ECS of the HF bioreactor, 1.42 mg Bio-AMS was infused for 60 min at a flow rate of 30 mL/h. This infusion was repeated on an almost daily basis for 18 days. Bio-AMS concentrations in HF samples were quantified by mass spectrometry as detailed below (see "Quantitation of Bio-AMS and biotin in mouse plasma") except that only 1 μL volumes of extracted samples were injected. PK analysis of drug concentrations attained in both CR (central reservoir) and ECS compartments was performed on days 0 and 14.

Statistical analysis:

Averages were used as a measure of central tendency. Data from continuous variables were analyzed using Mann-Whitney and Student's *t* tests. Differences with P less or equivalent to 0.05 were considered statistically significant. All statistical analyses were performed using GraphPad Prism 7.0 (GraphPad Software Inc.)

Supplementary Material

Refer to Web version on PubMed Central for supplementary material.

Acknowledgements

We thank Carolyn Bertozzi for providing the Rv3406 over-expression plasmid and Leila de Mendonca Lima Pesquisadora Titular for antiserum raised against Rv3406.

Funding

This work was supported by grants AI091790 (NIAID) and U19AI111143 (Tri-Institutional TB Research Unit, part of the NIAID TBRU Network) and OPP1154895 (BMGF).

Data and materials availability

All data supporting the findings of this study are presented in the manuscript. Whole genome sequences of Bio-AMS resistant *Mtb* isolates have been submitted to Genbank. The antiserum raised against Rv3406 was obtained from Dr. Leila de Mendonca Lima Pesquisadora Titular under a material transfer agreement (MTA) between Weill Cornell Medical College and the Oswaldo Cruz Foundation (FIOCRUZ). The Rv3406 overexpression plasmid was obtained from Dr. Bertozzi under an MTA between UC Berkeley and the Regents of the University of Minnesota. Reagents derived from the work will be available upon request through material transfer agreements.

References

1. W. H. Organization, Antimicrobial resistance: global report on surveillance. (World Health Organization, 2014).
2. Moliva JI, Turner J, Torrelles JB, Prospects in Mycobacterium bovis Bacille Calmette et Guerin (BCG) vaccine diversity and delivery: why does BCG fail to protect against tuberculosis? Vaccine 33, 5035–5041 (2015). [PubMed: 26319069]
3. Draper P, The outer parts of the mycobacterial envelope as permeability barriers. Front Biosci 3, D1253–1261 (1998). [PubMed: 9851911]
4. Morris RP, Nguyen L, Gatfield J, Visconti K, Nguyen K, Schnappinger D, Ehrt S, Liu Y, Heifets L, Pieters J, Schoolnik G, Thompson CJ, Ancestral antibiotic resistance in Mycobacterium tuberculosis. Proc Natl Acad Sci U S A 102, 12200–12205 (2005). [PubMed: 16103351]

5. Nguyen L, Pieters J, Mycobacterial subversion of chemotherapeutic reagents and host defense tactics: challenges in tuberculosis drug development. Annu Rev Pharmacol Toxicol 49, 427–453 (2009). [PubMed: 19281311]
6. Nguyen L, Thompson CJ, Foundations of antibiotic resistance in bacterial physiology: the mycobacterial paradigm. Trends Microbiol 14, 304–312 (2006). [PubMed: 16759863]
7. Jarlier V, Nikaido H, Mycobacterial cell wall: structure and role in natural resistance to antibiotics. FEMS Microbiol Lett 123, 11–18 (1994). [PubMed: 7988876]
8. Bazet Lyonnet B, Diacovich L, Cabruja M, Bardou F, Quemard A, Gago G, Gramajo H, Pleiotropic effect of AccD5 and AccE5 depletion in acyl-coenzyme A carboxylase activity and in lipid biosynthesis in mycobacteria. PLoS One 9, e99853 (2014). [PubMed: 24950047]
9. Kurth DG, Gago GM, de la Iglesia A, Bazet Lyonnet B, Lin TW, Morbidoni HR, Tsai SC, Gramajo H, ACCase 6 is the essential acetyl-CoA carboxylase involved in fatty acid and mycolic acid biosynthesis in mycobacteria. Microbiology 155, 2664–2675 (2009). [PubMed: 19423629]
10. Rainwater DL, Kolattukudy PE, Isolation and characterization of acyl coenzyme A carboxylases from Mycobacterium tuberculosis and Mycobacterium bovis, which produce multiple methyl-branched mycocerosic acids. J Bacteriol 151, 905–911 (1982). [PubMed: 6807964]
11. Oh TJ, Daniel J, Kim HJ, Sirakova TD, Kolattukudy PE, Identification and characterization of Rv3281 as a novel subunit of a biotin-dependent acyl-CoA Carboxylase in Mycobacterium tuberculosis H37Rv. J Biol Chem 281, 3899–3908 (2006). [PubMed: 16354663]
12. Park SW, Casalena DE, Wilson DJ, Dai R, Nag PP, Liu F, Boyce JP, Bittker JA, Schreiber SL, Finzel BC, Schnappinger D, Aldrich CC, Target-based identification of whole-cell active inhibitors of biotin biosynthesis in Mycobacterium tuberculosis. Chem Biol 22, 76–86 (2015). [PubMed: 25556942]
13. Dai R, Wilson DJ, Geders TW, Aldrich CC, Finzel BC, Inhibition of Mycobacterium tuberculosis transaminase BioA by aryl hydrazines and hydrazides. Chembiochem 15, 575–586 (2014). [PubMed: 24482078]
14. Shi C, Aldrich CC, Design and synthesis of potential mechanism-based inhibitors of the aminotransferase BioA involved in biotin biosynthesis. J Org Chem 77, 6051–6058 (2012). [PubMed: 22724679]
15. Shi C, Geders TW, Park SW, Wilson DJ, Boshoff HI, Abayomi O, Barry CE, 3rd, Schnappinger D, Finzel BC, Aldrich CC, Mechanism-based inactivation by aromatization of the transaminase BioA involved in biotin biosynthesis in Mycobaterium tuberculosis. J Am Chem Soc 133, 18194–18201 (2011). [PubMed: 21988601]
16. Shi C, Tiwari D, Wilson DJ, Seiler CL, Schnappinger D, Aldrich CC, Bisubstrate Inhibitors of Biotin Protein Ligase in Resistant to Cyclonucleoside Formation. ACS Med Chem Lett 4, (2013).
17. Duckworth BP, Geders TW, Tiwari D, Boshoff HI, Sibbald PA, Barry CE, 3rd, Schnappinger D, Finzel BC, Aldrich CC, Bisubstrate adenylation inhibitors of biotin protein ligase from Mycobacterium tuberculosis. Chem Biol 18, 1432–1441 (2011). [PubMed: 22118677]
18. Bockman MR, Kalinda AS, Petrelli R, De la Mora-Rey T, Tiwari D, Liu F, Dawadi S, Nandakumar M, Rhee KY, Schnappinger D, Finzel BC, Aldrich CC, Targeting Mycobacterium tuberculosis Biotin Protein Ligase (MtBPL) with Nucleoside-Based Bisubstrate Adenylation Inhibitors. J Med Chem 58, 7349–7369 (2015). [PubMed: 26299766]
19. Purushothaman S, Gupta G, Srivastava R, Ramu VG, Surolia A, Ligand specificity of group I biotin protein ligase of Mycobacterium tuberculosis. PLoS One 3, e2320 (2008). [PubMed: 18509457]
20. Vilcheze C, Jacobs WR, Jr., The mechanism of isoniazid killing: clarity through the scope of genetics. Annu Rev Microbiol 61, 35–50 (2007). [PubMed: 18035606]
21. Pethe K, Sequeira PC, Agarwalla S, Rhee K, Kuhen K, Phong WY, Patel V, Beer D, Walker JR, Duraiswamy J, Jiricek J, Keller TH, Chatterjee A, Tan MP, Ujjini M, Rao SP, Camacho L, Bifani P, Mak PA, Ma I, Barnes SW, Chen Z, Plouffe D, Thayalan P, Ng SH, Au M, Lee BH, Tan BH, Ravindran S, Nanjundappa M, Lin X, Goh A, Lakshminarayana SB, Shoen C, Cynamon M, Kreiswirth B, Dartois V, Peters EC, Glynne R, Brenner S, Dick T, A chemical genetic screen in Mycobacterium tuberculosis identifies carbon-source-dependent growth inhibitors devoid of in vivo efficacy. Nat Commun 1, 57 (2010). [PubMed: 20975714]

22. Galvao TC, Lima CR, Gomes LH, Pagani TD, Ferreira MA, Goncalves AS, Correa PR, Degrave WM, Mendonca-Lima L, The BCG Moreau RD16 deletion inactivates a repressor reshaping transcription of an adjacent gene. Tuberculosis (Edinb) 94, 26–33 (2014). [PubMed: 24332305]
23. Sogi KM, Gartner ZJ, Breidenbach MA, Appel MJ, Schelle MW, Bertozzi CR, Mycobacterium tuberculosis Rv3406 is a type II alkyl sulfatase capable of sulfate scavenging. PLoS One 8, e65080 (2013). [PubMed: 23762287]
24. Srivastava S, Gumbo T, In vitro and in vivo modeling of tuberculosis drugs and its impact on optimization of doses and regimens. Curr Pharm Des 17, 2881–2888 (2011). [PubMed: 21834761]
25. Egelund EF, Alsultan A, Peloquin CA, Optimizing the clinical pharmacology of tuberculosis medications. Clin Pharmacol Ther 98, 387–393 (2015). [PubMed: 26138226]
26. Dartois V, Barry CE, Clinical pharmacology and lesion penetrating properties of second-and third-line antituberculous agents used in the management of multidrug-resistant (MDR) and extensively-drug resistant (XDR) tuberculosis. Curr Clin Pharmacol 5, 96–114 (2010). [PubMed: 20156156]
27. Schnappinger D, O'Brien KM, Ehrt S, Construction of conditional knockdown mutants in mycobacteria. Methods Mol Biol 1285, 151–175 (2015). [PubMed: 25779315]
28. Kim JH, O'Brien KM, Sharma R, Boshoff HI, Rehren G, Chakraborty S, Wallach JB, Monteleone M, Wilson DJ, Aldrich CC, Barry CE, 3rd, Rhee KY, Ehrt S, Schnappinger D, A genetic strategy to identify targets for the development of drugs that prevent bacterial persistence. Proc Natl Acad Sci U S A 110, 19095–19100 (2013). [PubMed: 24191058]
29. Woong Park S, Klotzsche M, Wilson DJ, Boshoff HI, Eoh H, Manjunatha U, Blumenthal A, Rhee K, Barry CE, 3rd, Aldrich CC, Ehrt S, Schnappinger D, Evaluating the sensitivity of Mycobacterium tuberculosis to biotin deprivation using regulated gene expression. PLoS Pathog 7, e1002264 (2011). [PubMed: 21980288]
30. Nikonenko BV, Protopopova M, Samala R, Einck L, Nacy CA, Drug therapy of experimental tuberculosis (TB): improved outcome by combining SQ109, a new diamine antibiotic, with existing TB drugs. Antimicrob Agents Chemother 51, 1563–1565 (2007). [PubMed: 17242141]
31. Nuermberger EL, in Antituberculosis Chemotherapy, Donald PR, Helden PD, Eds. (Karger AG, Basel, 2011), chap. 15, pp. 145–152.
32. Karakousis PC, Yoshimatsu T, Lamichhane G, Woolwine SC, Nuermberger EL, Grosset J, Bishai WR, Dormancy phenotype displayed by extracellular Mycobacterium tuberculosis within artificial granulomas in mice. J Exp Med 200, 647–657 (2004). [PubMed: 15353557]
33. Gill WP, Harik NS, Whiddon MR, Liao RP, Mittler JE, Sherman DR, A replication clock for Mycobacterium tuberculosis. Nat Med 15, 211–214 (2009). [PubMed: 19182798]
34. Kruh NA, Troudt J, Izzo A, Prenni J, Dobos KM, Portrait of a pathogen: the Mycobacterium tuberculosis proteome in vivo. PLoS One 5, e13938 (2010). [PubMed: 21085642]
35. Neres J, Hartkoorn RC, Chiarelli LR, Gadupudi R, Pasca MR, Mori G, Venturelli A, Savina S, Makarov V, Kolly GS, Molteni E, Binda C, Dhar N, Ferrari S, Brodin P, Delorme V, Landry V, de Jesus Lopes Ribeiro AL, Farina D, Saxena P, Pojer F, Carta A, Luciani R, Porta A, Zanoni G, De Rossi E, Costi MP, Riccardi G, Cole ST, 2-Carboxyquinoxalines kill mycobacterium tuberculosis through noncovalent inhibition of DprE1. ACS Chem Biol 10, 705–714 (2015). [PubMed: 25427196]
36. J. T. C. o. t. B. T. Society, Chemotherapy and management of tuberculosis in the United Kingdom: recommendations 1998. Joint Tuberculosis Committee of the British Thoracic Society. Thorax 53, 536–548 (1998). [PubMed: 9797751]
37. Ormerod LP, Multidrug-resistant tuberculosis (MDR-TB): epidemiology, prevention and treatment. Br Med Bull 73-74, 17–24 (2005). [PubMed: 15956357]
38. Mitchison DA, Role of individual drugs in the chemotherapy of tuberculosis. Int J Tuberc Lung Dis 4, 796–806 (2000). [PubMed: 10985648]
39. Lin K, O'Brien KM, Trujillo C, Wang R, Wallach JB, Schnappinger D, Ehrt S, Mycobacterium tuberculosis Thioredoxin Reductase Is Essential for Thiol Redox Homeostasis but Plays a Minor Role in Antioxidant Defense. PLoS Pathog 12, e1005675 (2016). [PubMed: 27249779]

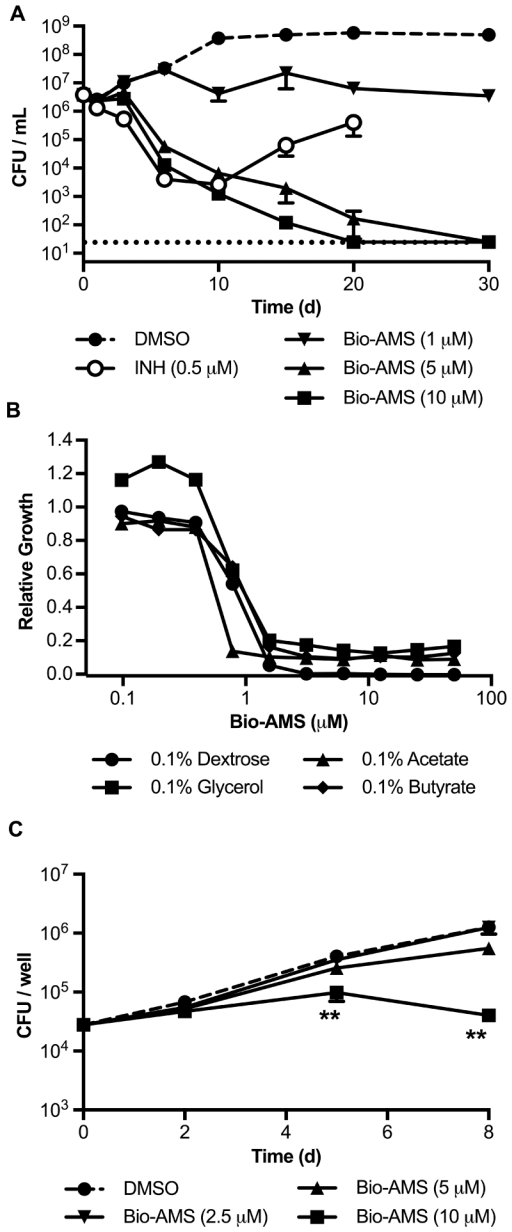

Fig. 1. Chemical inactivation of BPL kills Mtb and prevents growth in macrophages.

: (**A**) Impact of Bio-AMS on viability of *Mtb* in standard liquid culture. The dashed line indicates the limit of detection. (**B**) Impact of Bio-AMS on growth of *Mtb* with different carbon sources. Relative growth was calculated by dividing OD580 of the culture with Bio-AMS by the OD580 of the culture without Bio-AMS. (**C**) Impact of BioAMS on intracellular *Mtb*. Mouse bone marrow derived macrophages were infected and Bio-AMS or DMSO were added 24 h post infection. Data are representative of two independent experiments and averages 3 ± SEM (** P<0.01, Student's t-test)

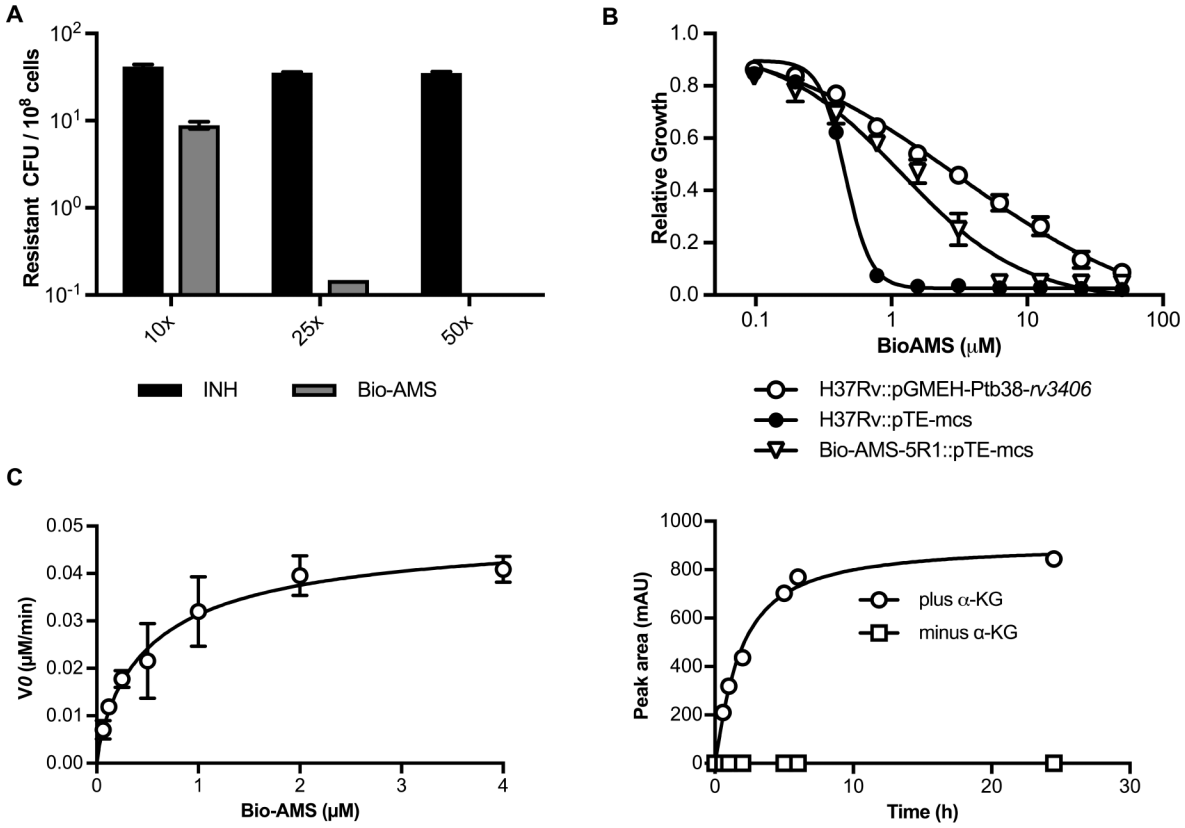

Fig. 2. Bio-AMS resistance

(**A**) Frequency of spontaneous resistance with Bio-AMS at concentrations of 1×, 25× and 50× the MIC. (**B**) Overexpression of Rv3406 causes resistance to Bio-AMS. H37Rv either contained the vector control (pTE-mcs) or the overexpression plasmid pGMEH-Ptb38-rv3406. One spontaneously resistant isolate (Bio-AMS-5R1) was included as a control. (**C**) Saturation curve used to determine the kinetic parameters for Bio-AMS oxidation by Rv3406. Data were fitted by non-linear regression to the Michaelis-Menten equation (left panel). Time course for Rv3406 catalyzed formation of UV active metabolite 3 as monitored by HPLC (right panel).

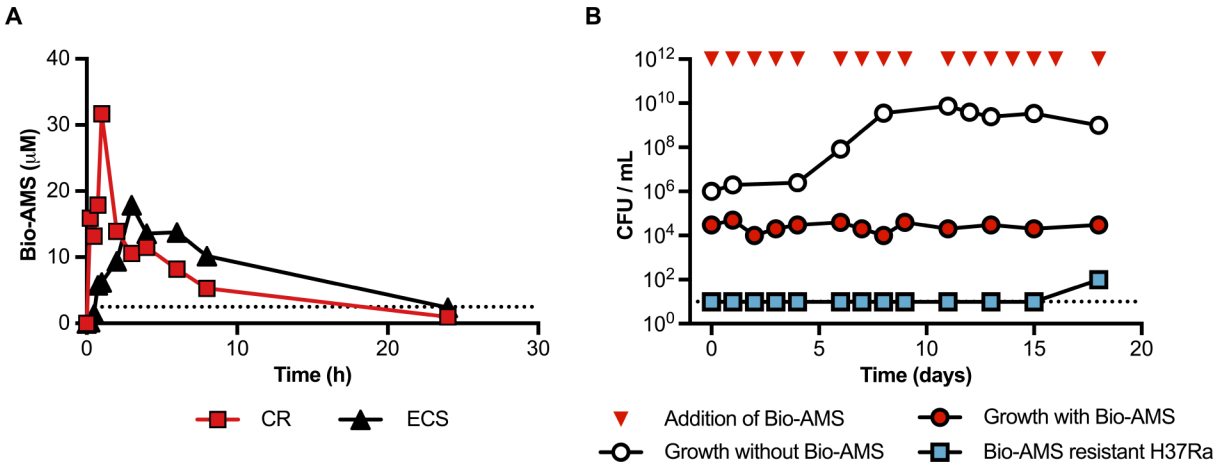

Fig. 3. Activity of Bio-AMS in a HFS

(**A**) Pharmacokinetic profile of Bio-AMS. Bio-AMS concentrations were measured in samples taken from the central reservoir (CR) and the extracapillary space (ECS). The dotted line represents the MIC90 of Bio-AMS for H37Ra. (**B**) Impact of Bio-AMS on viability of H37Ra. The dotted line indicates the lower limit of detection.

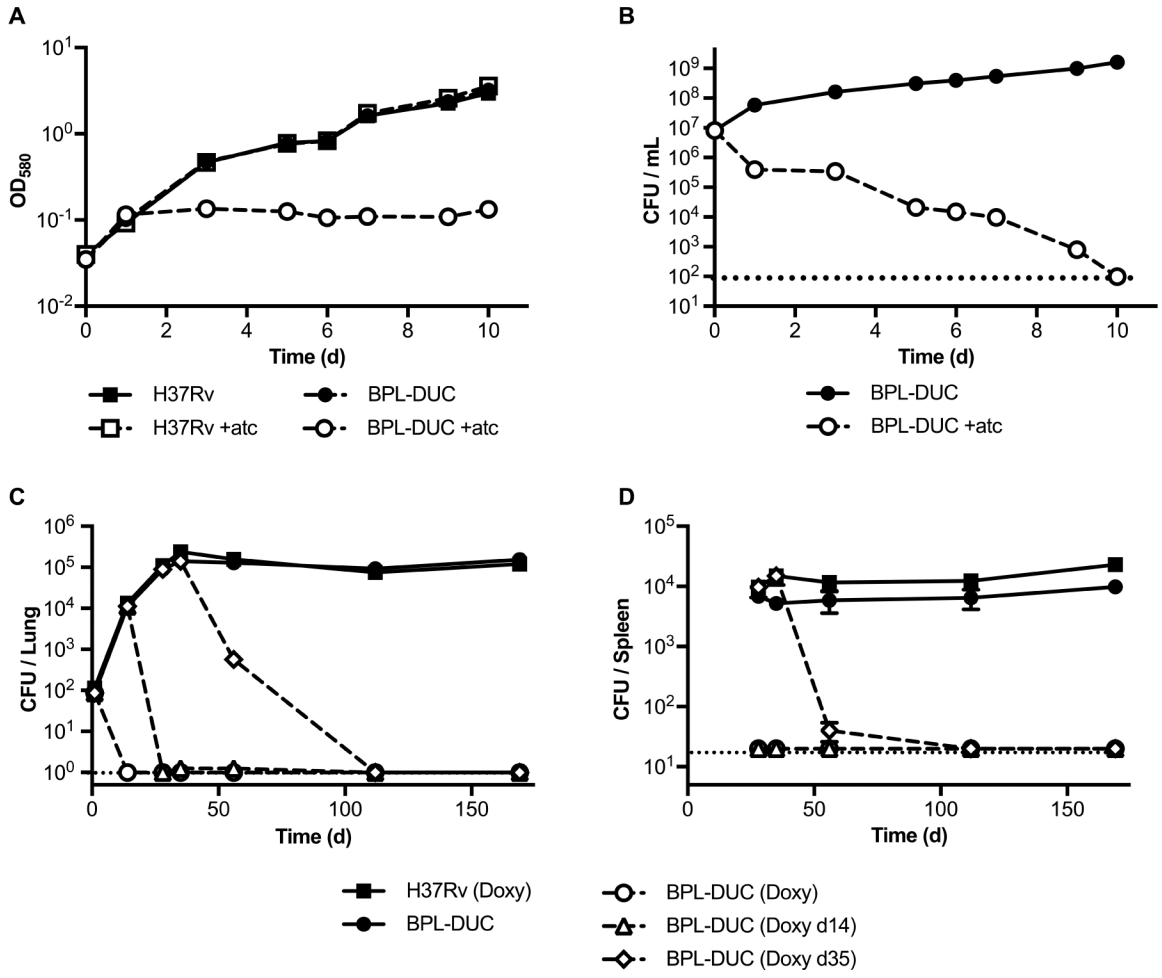

Fig. 4. Consequences of depleting BPL

Impact of BPL depletion on growth (**A**) and survival (**B**) in liquid media, mouse lungs (**C**), and spleens (**D**). Data are representative of three (A, B) or two (C, D) two independent experiments and averages of three (A, B) or four (C, D) samples ± SEM.

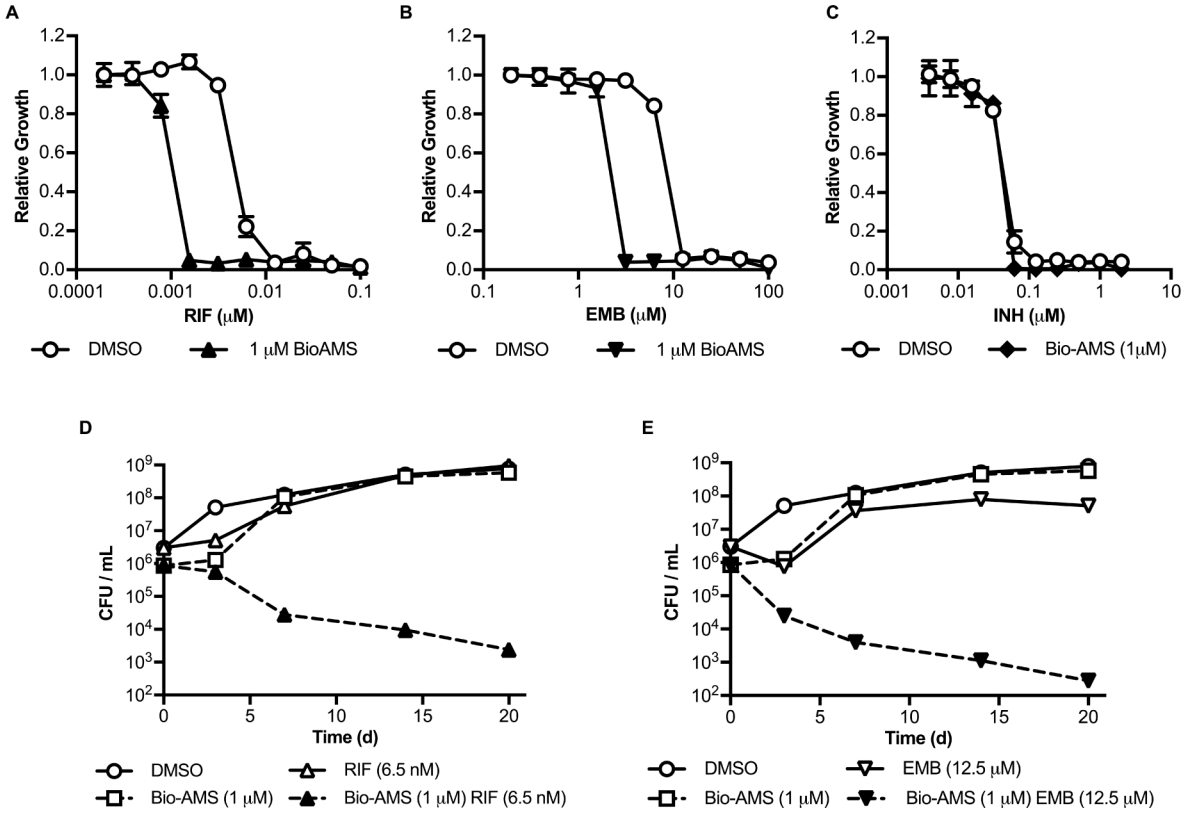

Fig. 5. Bio-AMS enhances the activity of rifampicin and ethambutol

Impact of Bio-AMS on the activities of RIF (**A**, **D**), EMB (**B**, **E**) and INH (**C**). Mtb was grown with Bio-AMS (1 μM in DMSO) or DMSO only for 3 days after which the bacteria were exposed to the other drugs. Data are representative of two independent experiments and averages of three ± SEM.

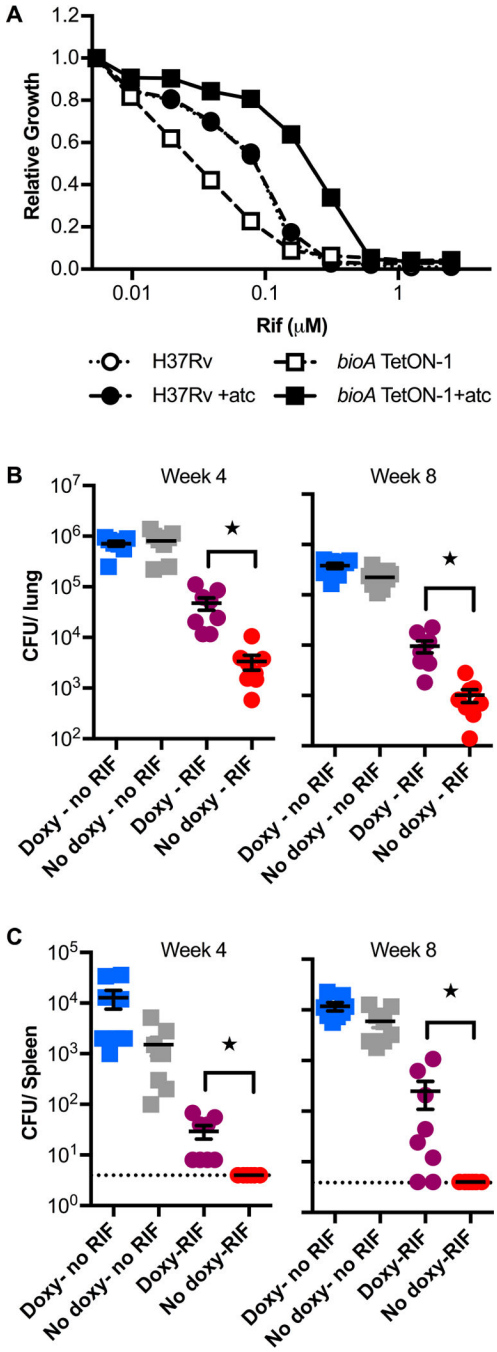

Fig. 6. Partial inhibition of biotin synthesis increases susceptibility of *Mtb* to RIF

Susceptibility of *bioA* TetON-1 to RIF *in vitro* (**A**) and during mouse infection (**B**, **C**). Data in B and C are means from eight mice ± SEM (* P<0.05, Mann Whitney test).